Use of ^{18}F-FDG PET/CT to differentiate ectopic adrenocorticotropic hormone-secreting lung tumors from tumor-like pulmonary infections in patients with ectopic Cushing syndrome

Guozhu Hou
Peking Union Medical College Hospital Chinese Academy of Medical Sciences and Peking Union Medical College

Yuanyuan Jiang
Peking Union Medical College Hospital Chinese Academy of Medical Sciences and Peking Union Medical College

Fang Li
Peking Union Medical College Hospital Chinese Academy of Medical Sciences and Peking Union Medical College

Xin Cheng (chengx@pumch.cn)
Peking Union Medical College Hospital Chinese Academy of Medical Sciences and Peking Union Medical College

---

Research Article

Keywords: ectopic Cushing syndrome, adrenocorticotropic hormone-secreting lung tumors, pulmonary infections, fluorodeoxyglucose, positron emission tomography/computed tomography

Posted Date: April 15th, 2021

DOI: https://doi.org/10.21203/rs.3.rs-403749/v1

Abstract

Background: Ectopic adrenocorticotropic hormone (ACTH)-secreting lung tumors represent the most common cause of ectopic Cushing syndrome (ECS). Pulmonary opportunistic infections are associated with ECS and occasionally difficult to differentiate from tumors by using computed tomography (CT) alone. The present study aimed to evaluate the usefulness of ^{18}F-fluorodeoxyglucose (FDG) positron emission tomography/CT (^{18}F-FDG PET/CT) for differentiating ectopic ACTH-secreting lung tumors from tumor-like pulmonary infections in patients with ECS.

Methods: We retrospectively reviewed the imaging data for 24 patients with ECS who were suspected to have ACTH-secreting lung tumors and underwent ^{18}F-FDG PET/CT between 2008 and 2019. Part of the 24 patients underwent ^{99m}Tc-HYNIC-TOC scintigraphy and ^{68}Ga-DOTA-TATE PET/CT.

Results: In total, 18 patients had lung tumors and six had pulmonary infections. The primary source of ECS remained occult in the six patients with pulmonary infections. The maximum standardized uptake value (SUV_{max}) for pulmonary infections was significantly higher than that for tumors (P = 0.008). Receiver operating characteristic analysis was performed, and it was found that a cut-off SUV_{max} of 4.95 helped in differentiating lung tumors from infections with 75% sensitivity and 94.4% specificity. In a subgroup analysis of 12 typical and five atypical carcinoids, there was no significant between-group difference with respect to SUV_{max}, the lesion size, the ACTH level, and the prevalence of regional lymph node metastasis. Four out of 6 patients with 5 infectious lesions and 16 out of 18 patients with 16 ACTH-secreting tumors underwent ^{99m}Tc-HYNIC-TOC scintigraphy, and 1/6 patients with 1 infectious lesion, and 6 out of 18 patients with 6 ACTH-secreting tumors underwent ^{68}Ga-DOTA-TATE PET/CT. There is no significant difference in sensitivity between tumor lesions and infections using ^{99m}Tc-HYNIC-TOC scintigraphy.

Conclusions: Our findings suggest that pulmonary infections exhibit significantly higher FDG uptake than do well-differentiated ACTH-secreting lung tumors in ^{18}F-FDG PET/CT. Therefore, SUV_{max} (cut-off 4.95) may be useful for differentiating the two conditions. However, ^{99m}Tc-HYNIC-TOC scintigraphy is of no value in distinguishing the focus of well-differentiated ACTH-secreting lung tumors from that of infection. Typical and atypical ACTH-secreting lung carcinoids may show similar clinical behavior and appearance on ^{18}F-FDG PET/CT.

Background

10%-15% of Cushing syndrome is caused by ectopic adrenocorticotropic hormone (ACTH)-secreting tumors. In such cases, resection of the tumors can have curative effects. The most common tumors associated with ECS are pulmonary carcinoids and small cell lung carcinoma (SCLC), followed by thymic carcinoids, pancreatic neuroendocrine tumors, medullary thyroid carcinoma, and pheochromocytoma [1]. ^{18}F-fluorodeoxyglucose (FDG) positron emission tomography (PET)/computed tomography (CT; ^{18}F-FDG

PET/CT) has been shown to be an effective modality for localizing ectopic ACTH-secreting tumors causing ECS. Pulmonary carcinoids generally demonstrate low to moderate metabolic activity because of their low proliferation rate and slow growth. Meanwhile, ACTH-producing SCLC can show positive findings on ^{18}F-FDG PET/CT, although the reported number of ECS-causing SCLCs detected by ^{18}F-FDG PET/CT is quite small. This is probably because the patients are rapidly diagnosed by conventional cross-sectional imaging and do not undergo ^{18}F-FDG PET/CT for source localization [2].

ECS due to ectopic ACTH-secreting tumors is associated with markedly elevated ACTH levels. This results in high circulating glucocorticoid levels, which primarily affect cell-mediated immunity [3] and impair immune function by inhibiting the phagocytic function of alveolar macrophages and reducing neutrophil recruitment to the infected areas. This results in an increased incidence of opportunistic bacterial and fungal infections [4, 5]. The four most common infections associated with ECS are cryptococcosis, aspergillosis, nocardiosis, and pneumocystosis [6], with the lung being the most frequently involved site. Pulmonary infections can exhibit varied radiographic findings and may appear as nodules or masses simulating lung tumors [7]. Thus, it could be difficult to differentiate tumor-like pulmonary infections from lung tumors by using conventional cross-sectional imaging. FDG is a nonspecific tracer that accumulates in areas of infection. Pulmonary cryptococcosis, aspergillosis, nocardiosis, and pneumocystosis have been reported to show high metabolic activity and mimic lung malignancies on ^{18}F-FDG PET/CT [8–11].

In the setting of immunosuppression resulting from ECS, surgery for the removal of pulmonary infectious lesions misdiagnosed as ectopic ACTH-secreting tumors can deteriorate the patient's condition. Therefore, discrimination of infections and tumors is crucial for avoiding unnecessary surgical intervention. The primary goal of this retrospective study was to evaluate the usefulness of ^{18}F-FDG PET/CT for differentiating ectopic ACTH-secreting lung tumors from tumor-like pulmonary infections in patients with ECS.

Materials And Methods

Patients

We retrospectively reviewed ^{18}F-FDG PET/CT scans obtained for localizing the source of ectopic ACTH secretion in all patients with ECS in our department between 2008 and 2019. Eventually, 24 patients with suspicious ACTH-secreting lung tumors were included in the present study. The diagnosis of ECS was confirmed by clinical presentations combined with laboratory tests including low-dose dexamethasone suppression test (LDDST), high-dose dexamethasone suppression test (HDDST), CRH test, inferior petrosal sinus sampling (IPSS). The head MRI results of all patients suggested that the pituitary gland was normal. Pulmonary CT indicates pulmonary nodules, but the nature is unclear. The reference standard was histopathological diagnosis obtained by either lung surgery or biopsy. There were 11 female and 13 male patients aged 9 to 72 years (mean age, 37.8 ± 17.1 years).

This study was conducted in accordance with the Declaration of Helsinki. This retrospective study of existing patient data and images was approved by the institutional review board of Peking Union Medical College Hospital. The requirement for informed consent was waived.

^{99m}Tc-HYNIC-TOC scintigraphy

^{99m}Tc-HYNIC-TOC was synthesized and labeled as previously described[12]. After intravenous administration of the tracer, whole-body planar images were acquired using a double-head gamma camera at 1 and 4 hours after injection. Some patients also underwent pulmonary SPECT/CT imaging when there is an increased uptake in the chest.

^{18}F-FDG PET/CT Study

Following 8 h of fasting and confirming the blood glucose level to be less than 120 mg/dL, ^{18}F-FDG (5.5 MBq/kg) was intravenously injected. An hour later, PET/CT images were acquired from the mid-thigh to the skull base (2 min/bed position) using a combined PET/CT Biograph (Siemens Co.). All scans were obtained in a three-dimensional model.

^{68}Ga-DOTA-TATE PET/CT Study

The ^{68}Ga-DOTATATE was produced following our previously published procedure[13]. The study was carried out on a PET/CT scanner (Siemens Co.). Patients received an intravenous injection of ^{68}Ga-DOTATATE (111–148 MBq). A low-dose whole-body CT scan was obtained at 40–60 min post-injection for anatomical localization and attenuation correction. PET scanning followed at 1.5 min/bed position with a 23-slice overlap. Images were reconstructed using an ordered subsets expectation-maximization algorithm and corrected for CT-based attenuation, dead time, random events, and scatter.

Image interpretation and statistical analysis

The PET/CT scans were reviewed by two experienced nuclear medicine physicians, who visually inspected the images and performed semi-quantitative measurements based on the maximum standard uptake value (SUV_{max}), which is determined by selecting the point of maximum FDG uptake within the lesion. The intensity of tumor uptake and ^{99m}Tc-HYNIC-TOC scintigraphy was graded on a scale from 0 to 3 by comparing them with the tracer uptake intensity of the normal liver (0: background activity, negative scan; 1: mild uptake, abnormal uptake higher than the background but less than that in the normal liver; 2: moderate uptake, abnormal uptake equal to that in the normal liver; and 3: intense uptake, abnormal uptake greater than that in the normal liver). Tumors with a score of 1, 2, or 3 were considered positive. The uptake and anatomical changes of suspicious sites on ^{68}Ga-DOTA-TATE PET/CT were recorded and analyzed. The high-intensity uptake is defined as the uptake of the focus that is significantly higher than that of the surrounding tissue.

All data are expressed as mean ± standard deviation. Differences between groups were analyzed using the Student *t* test, nonparametric analysis, and $\chi 2$ test. The cut-off SUV_{max} for differentiating pulmonary

infections from ACTH-secreting tumors was obtained via receiver operating characteristic (ROC) analysis with calculation of areas under the curve (AUCs) and sensitivity and specificity values. A *P*-value of < 0.05 was considered statistically significant. All statistical analyses were performed using SPSS Statistics (version 21.0, IBM SPSS Inc., IBM, Chicago, IL, USA).

Results

Among the 24 patients, 18 patients with 18 lesions were diagnosed with ectopic ACTH-secreting tumours (typical carcinoids, n = 12; atypical carcinoids, n = 5; SCLC, n = 1) while six patients with eight lesions were diagnosed with pulmonary infections (cryptococcosis, n = 3; aspergillosis, n = 4; pulmonary abscess, n = 1). Therefore, a total of 26 lesions were analyzed in this study. The patient characteristics are shown in Table 1. After surgical resection of the lesions, all patients in the tumor group were relieved of all symptoms, with serum cortisol and ACTH levels returning to normal. On the other hand, the source of ectopic ACTH secretion remained occult in patients with pulmonary infections. The mean SUV_{max} for all 18 lesions in the patients with ectopic ACTH-secreting lung tumors was 2.1 ± 1.8 (range: 0.6–7.7), while that for the eight lesions in the patients with pulmonary infections was 5.9 ± 3.8 (range: 1.0–12.4). Thus, SUV_{max} was significantly higher for infectious lesions than for tumors ($P = 0.008$; Fig. 1). ROC curve analysis suggested that an SUV_{max} of ≥ 4.95 was predictive of pulmonary infection with 75% sensitivity and 94.4% specificity; AUC was 0.833 (standard error, 0.093; $P = 0.008$; 95% confidence interval, 0.651–1.000; Fig. 2). The mean diameters of the ectopic ACTH-secreting lung tumors and pulmonary infectious lesions were 13.8 ± 7.9 (range: 5–37) and 20.9 ± 11.0 (range: 7–35) mm, respectively, with no significant between-group difference ($P = 0.126$; Table 2). Figures 3, 4, 5, 6, and 7 present representative cases of cryptococcosis (two lesions; SUV_{max}, 5.7 and 12.4), aspergillosis (SUV_{max}, 1.0), an atypical carcinoid (SUV_{max}, 1.1), a typical carcinoid (SUV_{max}, 2.8), and small cell lung cancer (SUV_{max}, 7.7), respectively.

Table 1
Clinical features of ectopic Cushing syndrome patients, including pathology, metastases, size, and SUV_{max} of lesions

Patient	Sex/age	ACTH (pg/ml)*	Pathology	Metastases	Diameter (mm)	SUV_{max}
Infectious lesions						
1	F/60	326	cryptococcus	N/A	7	1.2
2	F/41	59.1	Abscess	N/A	32	6.2
3	F/34	49.5	cryptococcus	N/A	14	5.7
3	F/34	49.5	cryptococcus	N/A	35	12.4
4	M/39	48.5	Aspergillus	N/A	23	1.0
5	M/53	1041	Aspergillus	N/A	32	9.7
5	M/53	1041	Aspergillus	N/A	12	5.2
6	F/47	N/A	Aspergillus	N/A	12	5.8
ACTH-secreting tumors						
7	M/28	191	TC	-	10	0.6
8	M/29	116	TC	-	12	4.7
9	F/9	115	AC	-	14	1.4
10	M/24	222	TC	+	17	2.7
11	F/48	153	TC	-	5	0.8
12	F/27	111	TC	-	8	0.9
13	M/22	140	AC	-	6	0.9
14	M/13	107	TC	+	10	1.1
15	M/45	68.3	AC	+	10	1.9
16	M/30	100	TC	-	11	0.6
17	F/72	129	TC	-	15	2.8
18	F/44	874	TC	+	9	0.7
19	F/45	60.6	TC	+	16	3.8
20	F/52	572	TC	+	14	3.4

SUV_{max}, maximum standardized uptake value; N/A, not applicable; AC, atypical carcinoid; TC, typical carcinoid; F, female; M, male; SCLC, small cell lung cancer. * Reference range for ACTH: 0–46 pg/ml.

Patient	Sex/age	ACTH (pg/ml)*	Pathology	Metastases	Diameter (mm)	SUV_{max}
21	M/16	130	AC	-	19	1.1
22	M/12	865	AC	+	28	3.0
23	M/62	278	TC	-	7	0.6
24	M/57	261	SCLC	+	37	7.7

SUV_{max}, maximum standardized uptake value; N/A, not applicable; AC, atypical carcinoid; TC, typical carcinoid; F, female; M, male; SCLC, small cell lung cancer. * Reference range for ACTH: 0–46 pg/ml.

Table 2
Imaging and clinical characteristics of ectopic Cushing syndrome patients

	ACTH-secreting tumors (n = 18)	Infectious lesions (n = 8)	*P* value
Diameter (mm)	13.8 ± 7.9 (5–37)	20.9 ± 11.0 (7–35)	0.126
SUV_{max}	2.1 ± 1.8 (0.6–7.7)	5.9 ± 3.8 (1.0-12.4)	0.008

SUV_{max}, maximum standardized uptake value

In a subgroup analysis of the 12 typical carcinoids and five atypical carcinoids, the mean SUV_{max} was 1.9 ± 1.5 and 1.6 ± 0.8 mm, respectively, with no significant between-group difference (P = 0.597; Fig. 8). Moreover, there were no significant differences between the typical and atypical groups in terms of the lesion size (11.1 ± 3.7 mm vs. 15.4 ± 8.5 mm, respectively; P = 0.165) and ACTH level (242.8 ± 240.8 pg/ml vs. 263.6 ± 337.3 pg/ml, respectively; P = 0.833). Five of the 12 typical carcinoids (41.7%) and two of the five atypical carcinoids (40%) were confirmed with hilar or mediastinal lymph node metastasis in the histopathological analysis (P = 0.951; Table 3). No distant metastases were detected on ^{18}F-FDG PET/CT in either group.

Table 3
Characteristics in subgroup analysis of typical carcinoids and atypical carcinoids

	TC	AC	*P* value
SUV_{max}	1.9 ± 1.5	1.6 ± 0.8	0.597
Diameter (mm)	11.1 ± 3.7	15.4 ± 8.5	0.165
ACTH level (pg/ml) *	242.8 ± 240.8	263.6 ± 337.3	0.833
lymph node metastasis	5/12 (41.7%)	2/5 (40%)	0.951

SUV_{max}, maximum standardized uptake value; AC, atypical carcinoid; TC, typical carcinoid; * Reference range for ACTH: 0–46 pg/ml.

In our retrospective study, 4 out of 6 patients with 5 infectious lesions and 16 out of 18 patients with 16 ACTH-secreting tumors underwent ^{99m}Tc-HYNIC-TOC scintigraphy, and 1/6 patients with 1 infectious lesion, and 6 out of 18 patients with 6 ACTH-secreting tumors underwent ^{68}Ga-DOTA-TATE PET/CT. There is no significant difference in sensitivity between tumor lesions and infections using ^{99m}Tc-HYNIC-TOC scintigraphy (18.75%, 3/16 vs. 40%, 2/5, respectively; $P = 0.553$; Fig. 9). For infectious lesions, the sensitivity of ^{68}Ga-DOTA-TATE PET/CT is 0% (0/1), and for tumor lesions, the sensitivity of ^{68}Ga-DOTA-TATE PET/CT is 83.3% (5/6). (Table 4)

Table 4

The ^{99m}Tc-HYNIC-TOC scintigraphy, ^{68}Ga-DOTA-TATE PET/CT, Pathological and Immunohistochemical results of ectopic Cushing syndrome patients

Patient	Sex/age	^{99m}Tc-HYNIC-TOC	^{68}Ga-DOTA-TATE	Histopathological characteristics
Infectious lesions				
1	F/60	N	N/A	cryptococcus
2	F/41	N	N/A	Abscess
3	F/34	P	N/A	cryptococcus
3	F/34	P	N/A	cryptococcus
4	M/39	N/A	N	Aspergillus
5	M/53	N/A	N/A	Aspergillus
5	M/53	N/A	N/A	Aspergillus
6	F/47	N	N/A	Aspergillus
ACTH-secreting tumors				
7	M/28	N	N/A	TC (ACTH, +; Ki-67, 1%; TTF-1, +)
8	M/29	N	N/A	TC (ACTH, +; Ki-67, 3%)
9	F/9	P	N/A	AC (ACTH, +; Number of mitosis, 1/10 HPF; Ki-67, 15%; TTF-1, -)
10	M/24	N	P	TC (ACTH, +; Ki-67, 3%; TTF-1, +)
11	F/48	N	N/A	TC (ACTH, +; Ki-67, 2%)
12	F/27	N	P	TC (ACTH, +; Ki-67, 3%)
13	M/22	N	P	AC (ACTH, +; Number of mitosis, 3/10 HPF; Ki-67, 6%)
14	M/13	N	P	TC (ACTH, +; Ki-67, 1%; TTF-1, +)
15	M/45	P	P	AC (ACTH, +; Number of mitosis, 8/10 HPF; Ki-67, 10%; TTF-1, +)
16	M/30	N	N/A	TC (ACTH, +; Number of mitosis, 1/10 HPF; Ki-67, 10%; TTF-1, +)
17	F/72	N	N/A	TC (ACTH, +; Ki-67, 2%; TTF-1, +)
18	F/44	N	N/A	TC (ACTH, +; Ki-67, 1%)

N or -, negative; P or +, positive; N/A, not applicable; AC, atypical carcinoid; TC, typical carcinoid; F, female; M, male; SCLC, small cell lung cancer; HPF, High Power Field.

Patient	Sex/age	^{99m}Tc-HYNIC-TOC	^{68}Ga-DOTA-TATE	Histopathological characteristics
19	F/45	N	N/A	TC (ACTH, +; Ki-67, 2%; TTF-1, +)
20	F/52	N	N	TC (ACTH, +; Ki-67, 2%; TTF-1, +)
21	M/16	N/A	N/A	AC (ACTH, +; Ki-67, 5%; TTF-1, +)
22	M/12	P	N/A	AC (ACTH, +; Ki-67, 2%)
23	M/62	N	N/A	TC (ACTH, +; Ki-67, 1%; TTF-1, +)
24	M/57	N/A	N/A	SCLC (ACTH, +; Ki-67, 25%)
N or -, negative; P or +, positive; N/A, not applicable; AC, atypical carcinoid; TC, typical carcinoid; F, female; M, male; SCLC, small cell lung cancer; HPF, High Power Field.				

The pathological and immunohistochemical results of ECS patients are listed in Table 4. All TC and AT are classified as well-differentiated neuroendocrine tumors (4 are graded G1, 13 are graded G2), and 1 SCLC is classified as poorly differentiated neuroendocrine tumors (G3). (Table 4)

Discussion

Ectopic ACTH-producing tumors account for 15–20% of cases of ACTH-dependent Cushing syndrome. Lung carcinoids and SCLC represent the most common tumors associated with ECS, and the resection of the responsible tumors can have curative effects [14]. There is no consensus regarding the usefulness of ^{18}F-FDG PET/CT for localizing the source of ectopic ACTH secretion, even though it is the most commonly used molecular imaging method in clinical practice because of its wide availability. A nodule or mass-like lesion in the lung that demonstrates abnormal activity on ^{18}F-FDG PET/CT, in the absence of abnormal lesions in other areas, tends to be interpreted as an ACTH-secreting tumor and is subjected to surgical resection. However, in clinical practice, the resected pulmonary ‘tumor’ occasionally turns out to be an infectious lesion most often caused by fungus. In such cases, surgery is unnecessary and can deteriorate the patient’s condition, considering the immunosuppression related to ECS. The present study included 18 patients with ectopic ACTH-secreting lung tumors and six patients with pulmonary infections. To the best of our knowledge, this is the first study to describe and compare the features of ACTH-secreting lung tumors and pulmonary infectious pseudotumors using ^{18}F-FDG PET/CT. This discrimination is important because the two conditions require entirely different treatment plans.

We found that a cut-off SUV_{max} of 4.95 maximized the sensitivity and specificity for the differentiation of pulmonary infections from ACTH-secreting tumors. Specifically, the findings indicated that a pulmonary nodule or mass-like lesion with a SUV_{max} of ≥ 4.95 was more likely to be an infectious lesion. Our study included only one SCLC, and it was the only lesion with a SUV_{max} of > 4.95 in the tumor group (SUV_{max}, 7.7). SCLCs generally exhibit high FDG uptake on PET/CT because of their aggressiveness and high

metabolic activity [15]. The SCLC was underrepresented in our series, probably because most SCLCs are rapidly diagnosed by conventional cross-sectional imaging and do not require ^{18}F-FDG PET/CT or other nuclear imaging modalities for localization [2]. ^{99m}Tc-HYNIC-TOC scintigraphy is of no value in distinguishing the focus of tumor from that of infection. Although 4 patients were negative in ^{99m}Tc-HYNIC-TOC scintigraphy and positive in ^{68}Ga-DOTA-TATE PET/CT, the number of cases was too small to clearly explain the value of ^{68}Ga-DOTA-TATE PET/CT. However, we can speculate that the sensitivity of ^{99m}Tc-HYNIC-TOC scintigraphy is lower than that of ^{68}Ga-DOTA-TATE PET/CT because ^{68}Ga-DOTA-TATE has a higher affinity for somatostatin receptor 2 (SSTR2) [16] and the spatial resolution of PET/CT is higher. In addition, inflammatory cells also express SSTR2[17], so the role of ^{99m}Tc-HYNIC-TOC scintigraphy and ^{68}Ga-DOTA-TATE PET/CT in the differentiation of ACTH-secreting tumours and pulmonary infections is not bright.

The present study showed significantly higher FDG accumulation in infectious lesions than in pulmonary carcinoids. The reason for the low FDG uptake of pulmonary carcinoids is that most of the lesions (17/18) are well-differentiated neuroendocrine neoplasms. [18] As mentioned in our preface, patients with poorly differentiated neuroendocrine neoplasms such as SCLC are rarely examined by FDG PET/CT, which is why we have fewer patients in this group. Among the eight infectious lesions, only two showed low FDG uptake with a SUV_{max} of < 4.95. One of the lesions (**Patient 1**, SUV_{max}, 1.2) was due to cryptococcosis, and it was the smallest lesion among the infectious pseudotumors (0.7 cm in diameter). The other infectious lesion with low FDG uptake was an aspergilloma (**Patient 4**, SUV_{max}, 1.0). Pulmonary aspergillosis can be divided into four subtypes on the basis of clinical and radiological findings: aspergilloma, allergic bronchopulmonary aspergillosis, chronic necrotizing aspergillosis, and invasive pulmonary aspergillosis (IPA) [19]. The first three subtypes are also considered to be non-invasive pulmonary aspergillosis (NIPA) [19]. Kim et al. evaluated the FDG PET/CT scans of 24 patients with pulmonary aspergillosis (8 IPA and 16 NIPA) and concluded that an isometabolic pattern on FDG PET/CT most likely represented NIPA [20]. NIPA is a chronic infection with low virulence and a mild inflammatory reaction, which might attribute to the low metabolic activity on ^{18}F-FDG PET/CT.

Pulmonary carcinoids are histologically classified into typical and atypical carcinoids. Some authors have reported that atypical carcinoids exhibited significantly higher FDG uptake than did typical carcinoids [21–24]. Tatci et al. also observed a higher SUV_{max} for atypical carcinoids than for typical carcinoids, although the difference was not statistically significant [25]. Fink et al analyzed the clinicopathological data and outcomes of 142 patients with pulmonary carcinoids (128 typical and 14 atypical) and found that atypical carcinoids were associated with higher rates of nodal involvement and distant metastases [26]. ACTH-secreting lung carcinoids are considered rare variants of pulmonary carcinoids, and ^{18}F-FDG PET/CT findings for these lesions have only been described in single case reports or small case series, with no study comparing typical and atypical carcinoids [27, 28]. In the present study, the mean SUV_{max} for atypical carcinoids was unexpectedly (although statistically insignificant) slightly lower than that for typical carcinoids. In addition, the prevalence of lymph node

involvement was similar in atypical carcinoids (40%) and typical carcinoids (41.7%). And we did not observe a significant difference between these two groups in terms of the lesion size, ACTH level neither. These results suggested that typical and atypical ACTH-secreting lung carcinoids exhibit similar clinical behavior and PET/CT findings, in contrast to previous findings concluding that atypical carcinoids generally exhibit higher FDG uptake, more aggressive behavior, and a worse prognosis [26]. We speculate that this discrepancy was caused by the fact that the pulmonary carcinoids enrolled in the previous studies did not show features of ectopic ACTH secretion.

The main limitations of this study were the small sample size, which does not allow for powerful statistical analysis, and retrospective design. In addition, survival and recurrence rates for ACTH-secreting carcinoids were not evaluated because of inadequate follow-up data. Therefore, a larger study is necessary to investigate whether the pathological subtype of ACTH-secreting lung carcinoids affects the clinical prognosis of these rare variants of pulmonary carcinoids. In the imaging diagnosis of neuroendocrine tumors, ^{18}F-FDG PET/CT and ^{68}Ga-DOTA-Peptides PET/CT are complementary. However, ^{68}Ga-DOTA-Peptides PET/CT is still in the preclinical stage in China, so not all patients suspected of having ECS undergo this examination. In our retrospective study, 7 patients (4#, 10#, 12#-15#, 20# showed in Table 1) underwent ^{68}Ga-DOTA-TATE PET/CT. The results showed that the lesions of Patient 4# and 20# were negative and the lesions of Patient 10#, 12#-15# lesions were positive. Because this data is very small, there is no value for discussion, and our study mainly wants to highlight the value of the auxiliary diagnosis of ^{18}F-FDG PET/CT, so the results of ^{68}Ga-DOTA-Peptides PET/CT are not discussed in this study.

Conclusion

In conclusion, although pulmonary infectious lesions associated with ECS and well-differentiated ACTH-secreting lung tumors occasionally exhibit similar morphological features, the former may show significantly higher FDG accumulation in ^{18}F-FDG PET/CT. Therefore, SUV_{max} (cut-off: 4.95) may be a useful parameter for differentiating the two conditions. However, ^{99m}Tc-HYNIC-TOC scintigraphy is of no value in distinguishing the focus of well-differentiated ACTH-secreting lung tumors from that of infection. Moreover, typical and atypical ACTH-secreting lung carcinoids may show similar clinical behavior and appearance on ^{18}F-FDG PET/CT. Further large-scale studies with adequate follow-up data are necessary to validate our findings.

Abbreviations

ACTH: adrenocorticotropic hormone; ECS: ectopic Cushing syndrome; CT: computed tomography; FDG: fluorodeoxyglucose; PET: positron emission tomography; SCLC: small cell lung carcinoma; SUV_{max}: the maximum standard uptake value; ROC: receiver operating characteristic; AUCs: areas under the curve; IPA: invasive pulmonary aspergillosis; NIPA: non-invasive pulmonary aspergillosis.

Declarations

Acknowledgements

We would like to thank *Editage* (www.editage.cn) for English language editing.

Authors' contributions

GH, YJ, FL, and XC contributed to the design and implementation of the research, to the analysis of the results, and to the writing of the manuscript. All authors contributed to the article and approved the submitted version.

Funding

This study was funded by CAMS Initiative for Innovative Medicine (CAMS-2018-I2M-3-001) and the National Natural Sciences Foundation of China (No.81201121).

Availability of data and materials

The dataset of the current study was available from the corresponding author on reasonable request.

Declarations

Ethics approval and consent to participate

This retrospective study of existing patient data and images was approved by the institutional review board of Peking Union Medical College Hospital. The requirement for informed consent was waived.

Consent for publication

Not applicable.

Competing interests

The authors declare that they have no conflict of interest.

Author details

[1] Department of Nuclear Medicine, Peking Union Medical College Hospital Chinese Academy of Medical Sciences and Peking Union Medical College, Beijing 100730, China

[2] Beijing Key Laboratory of Molecular Targeted Diagnosis and Therapy in Nuclear Medicine, Beijing 100730, China

Guozhu Hou and Yuanyuan Jiang contributed equally to this work

References

1. Ilias I, Torpy DJ, Pacak K, Mullen N, Wesley RA, Nieman LK. Cushing's syndrome due to ectopic corticotropin secretion: twenty years' experience at the National Institutes of Health. J Clin Endocrinol Metab. 2005;90:4955-62. doi:10.1210/jc.2004-2527.
2. Isidori AM, Sbardella E, Zatelli MC, Boschetti M, Vitale G, Colao A, et al. Conventional and Nuclear Medicine Imaging in Ectopic Cushing's Syndrome: A Systematic Review. J Clin Endocrinol Metab. 2015;100:3231-44. doi:10.1210/jc.2015-1589.
3. Auphan N, DiDonato JA, Rosette C, Helmberg A, Karin M. Immunosuppression by glucocorticoids: inhibition of NF-kappa B activity through induction of I kappa B synthesis. Science. 1995;270:286-90. doi:10.1126/science.270.5234.286.
4. Walsh TJ, Roilides E, Cortez K, Kottilil S, Bailey J, Lyman CA. Control, immunoregulation, and expression of innate pulmonary host defenses against Aspergillus fumigatus. Med Mycol. 2005;43 Suppl 1:S165-72. doi:10.1080/13693780500064672.
5. Stephens-Romero SD, Mednick AJ, Feldmesser M. The pathogenesis of fatal outcome in murine pulmonary aspergillosis depends on the neutrophil depletion strategy. Infect Immun. 2005;73:114-25. doi:10.1128/iai.73.1.114-125.2005.
6. Graham BS, Tucker WS, Jr. Opportunistic infections in endogenous Cushing's syndrome. Ann Intern Med. 1984;101:334-8. doi:10.7326/0003-4819-101-3-334.
7. Vanfleteren M, Dingemans AC, Surmont VF, Vermaelen KY, Postma AA, Oude Lashof AML, et al. Invasive Aspergillosis Mimicking Metastatic Lung Cancer. Front Oncol. 2018;8:188. doi:10.3389/fonc.2018.00188.
8. Mascarenhas NB, Lam D, Lynch GR, Fisher RE. PET imaging of cerebral and pulmonary Nocardia infection. Clin Nucl Med. 2006;31:131-3. doi:10.1097/01.rlu.0000200597.42832.39.
9. Huang CJ, You DL, Lee PI, Hsu LH, Liu CC, Shih CS, et al. Characteristics of integrated 18F-FDG PET/CT in Pulmonary Cryptococcosis. Acta Radiol. 2009;50:374-8. doi:10.1080/02841850902756532.
10. Sharma P, Mukherjee A, Karunanithi S, Bal C, Kumar R. Potential role of 18F-FDG PET/CT in patients with fungal infections. AJR Am J Roentgenol. 2014;203:180-9. doi:10.2214/ajr.13.11712.
11. Kono M, Yamashita H, Kubota K, Kano T, Mimori A. FDG PET Imaging in Pneumocystis Pneumonia. Clin Nucl Med. 2015;40:679-81. doi:10.1097/rlu.0000000000000831.
12. Decristoforo C, Melendez-Alafort L, Sosabowski JK, Mather SJ. 99mTc-HYNIC-[Tyr3]-octreotide for imaging somatostatin-receptor-positive tumors: preclinical evaluation and comparison with 111In-octreotide. J Nucl Med. 2000;41:1114-9.
13. Zhu W, Cheng Y, Wang X, Yao S, Bai C, Zhao H, et al. Head-to-Head Comparison of (68)Ga-DOTA-JR11 and (68)Ga-DOTATATE PET/CT in Patients with Metastatic, Well-Differentiated Neuroendocrine Tumors: A Prospective Study. J Nucl Med. 2020;61:897-903. doi:10.2967/jnumed.119.235093.

14. La Rosa S, Volante M, Uccella S, Maragliano R, Rapa I, Rotolo N, et al. ACTH-producing tumorlets and carcinoids of the lung: clinico-pathologic study of 63 cases and review of the literature. Virchows Arch. 2019;475:587-97. doi:10.1007/s00428-019-02612-x.
15. Kalemkerian GP. Small Cell Lung Cancer. Semin Respir Crit Care Med. 2016;37:783-96. doi:10.1055/s-0036-1592116.
16. Fani M, Nicolas GP, Wild D. Somatostatin Receptor Antagonists for Imaging and Therapy. J Nucl Med. 2017;58:61s-6s. doi:10.2967/jnumed.116.186783.
17. Elliott DE, Li J, Blum AM, Metwali A, Patel YC, Weinstock JV. SSTR2A is the dominant somatostatin receptor subtype expressed by inflammatory cells, is widely expressed and directly regulates T cell IFN-gamma release. Eur J Immunol. 1999;29:2454-63. doi:10.1002/(sici)1521-4141(199908)29:08<2454::Aid-immu2454>3.0.Co;2-h.
18. Panagiotidis E, Alshammari A, Michopoulou S, Skoura E, Naik K, Maragkoudakis E, et al. Comparison of the Impact of 68Ga-DOTATATE and 18F-FDG PET/CT on Clinical Management in Patients with Neuroendocrine Tumors. J Nucl Med. 2017;58:91-6. doi:10.2967/jnumed.116.178095.
19. Franquet T, Muller NL, Gimenez A, Guembe P, de La Torre J, Bague S. Spectrum of pulmonary aspergillosis: histologic, clinical, and radiologic findings. Radiographics. 2001;21:825-37. doi:10.1148/radiographics.21.4.g01jl03825.
20. Kim JY, Yoo JW, Oh M, Park SH, Shim TS, Choi YY, et al. (18)F-fluoro-2-deoxy-D-glucose positron emission tomography/computed tomography findings are different between invasive and noninvasive pulmonary aspergillosis. J Comput Assist Tomogr. 2013;37:596-601. doi:10.1097/RCT.0b013e318289aa31.
21. Jindal T, Kumar A, Venkitaraman B, Meena M, Kumar R, Malhotra A, et al. Evaluation of the role of [18F]FDG-PET/CT and [68Ga]DOTATOC-PET/CT in differentiating typical and atypical pulmonary carcinoids. Cancer Imaging. 2011;11:70-5. doi:10.1102/1470-7330.2011.0010.
22. Lococo F, Perotti G, Cardillo G, De Waure C, Filice A, Graziano P, et al. Multicenter comparison of 18F-FDG and 68Ga-DOTA-peptide PET/CT for pulmonary carcinoid. Clin Nucl Med. 2015;40:e183-9. doi:10.1097/rlu.0000000000000641.
23. Moore W, Freiberg E, Bishawi M, Halbreiner MS, Matthews R, Baram D, et al. FDG-PET imaging in patients with pulmonary carcinoid tumor. Clin Nucl Med. 2013;38:501-5. doi:10.1097/RLU.0b013e318279f0f5.
24. Kruger S, Buck AK, Blumstein NM, Pauls S, Schelzig H, Kropf C, et al. Use of integrated FDG PET/CT imaging in pulmonary carcinoid tumours. J Intern Med. 2006;260:545-50. doi:10.1111/j.1365-2796.2006.01729.x.
25. Tatci E, Ozmen O, Gokcek A, Biner IU, Ozaydin E, Kaya S, et al. 18F-FDG PET/CT rarely provides additional information other than primary tumor detection in patients with pulmonary carcinoid tumors. Ann Thorac Med. 2014;9:227-31. doi:10.4103/1817-1737.140134.
26. Fink G, Krelbaum T, Yellin A, Bendayan D, Saute M, Glazer M, et al. Pulmonary carcinoid: presentation, diagnosis, and outcome in 142 cases in Israel and review of 640 cases from the literature. Chest.

2001;119:1647-51. doi:10.1378/chest.119.6.1647.

27. Xu H, Zhang M, Zhai G, Zhang M, Ning G, Li B. The role of integrated (18)F-FDG PET/CT in identification of ectopic ACTH secretion tumors. Endocrine. 2009;36:385-91. doi:10.1007/s12020-009-9247-2.
28. Zhou J, Ju H, Zhu L, Pan Y, Lv J, Zhang Y. Value of fluorine-18-fluorodeoxyglucose PET/CT in localizing the primary lesion in adrenocorticotropic hormone-dependent Cushing syndrome. Nucl Med Commun. 2019;40:539-44. doi:10.1097/mnm.0000000000000989.

Figures

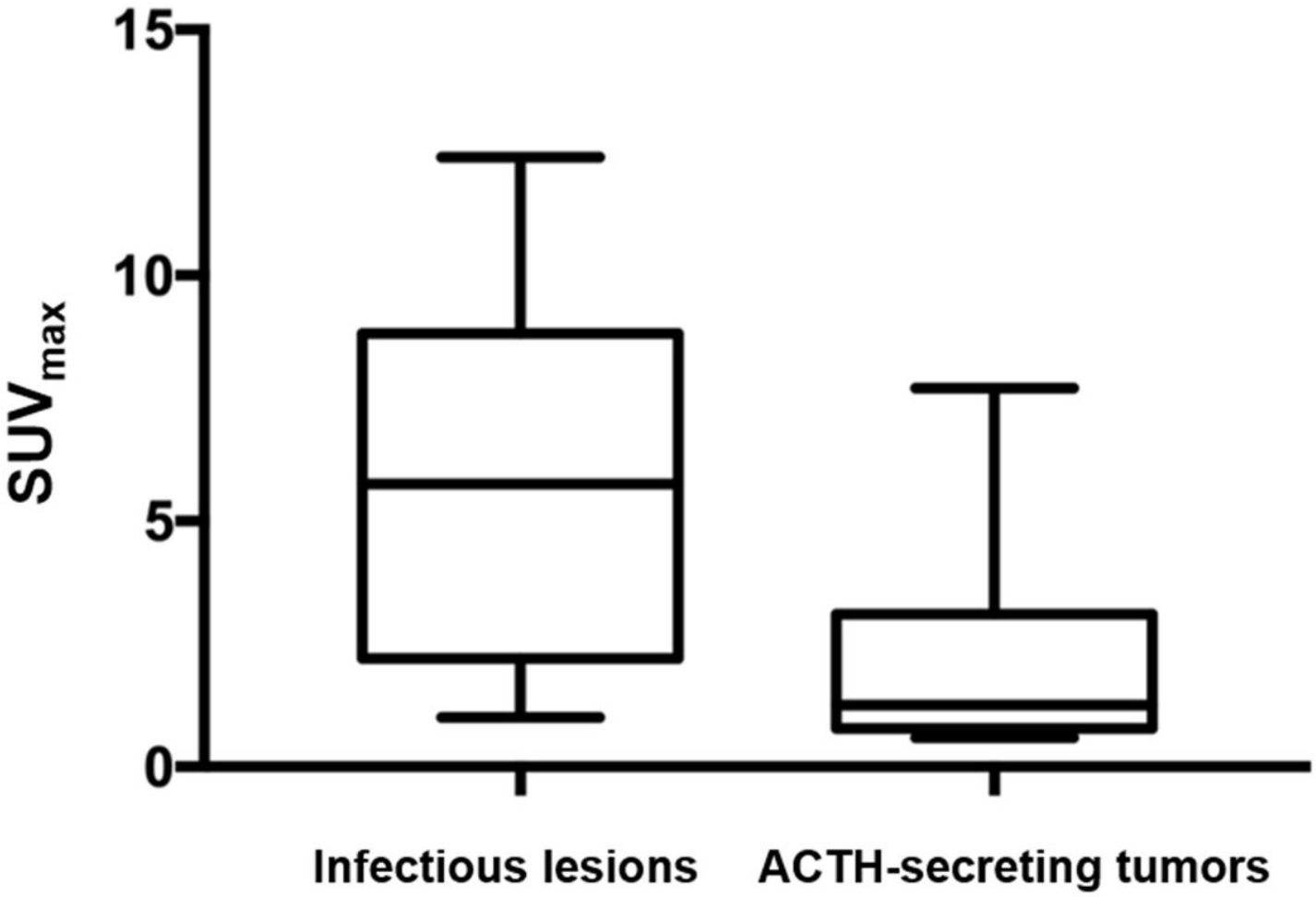

Figure 1

SUVmax was significantly higher for infectious lesions than for tumors (P = 0.008)

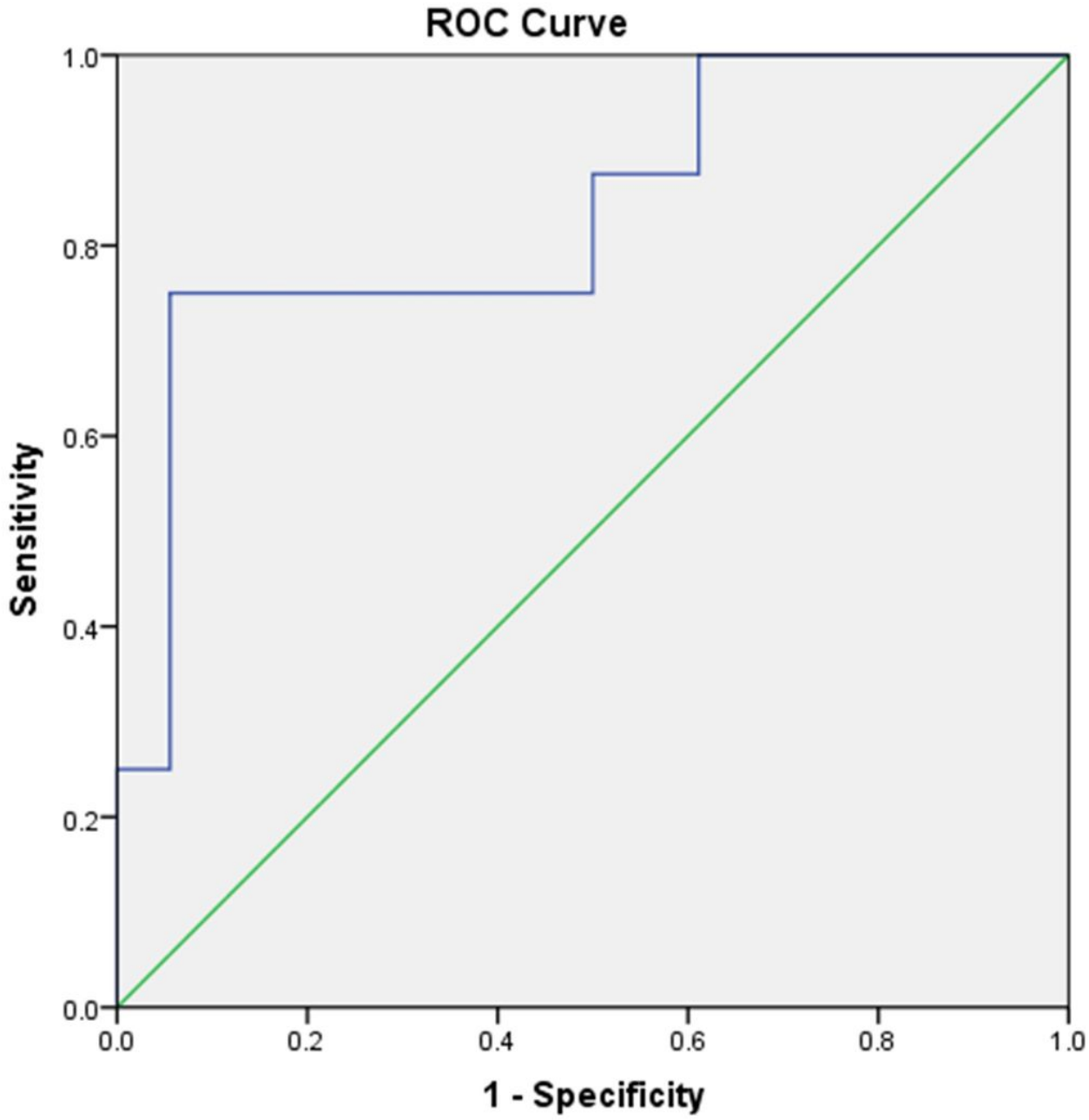

Figure 2

A receiver operating characteristic curve for measuring the accuracy of the SUVmax as a parameter for distinguishing pulmonary adrenocorticotropic hormone-secreting tumors from a pulmonary infection. The area under the curve is 0.833, with a cut-off point of 4.95 (standard error, 0.093; P=0.008; 95% confidence interval, 0.651–1.000). A SUVmax of 4.95 or greater is predictive of pulmonary infection with 75% sensitivity and 94.4% specificity.

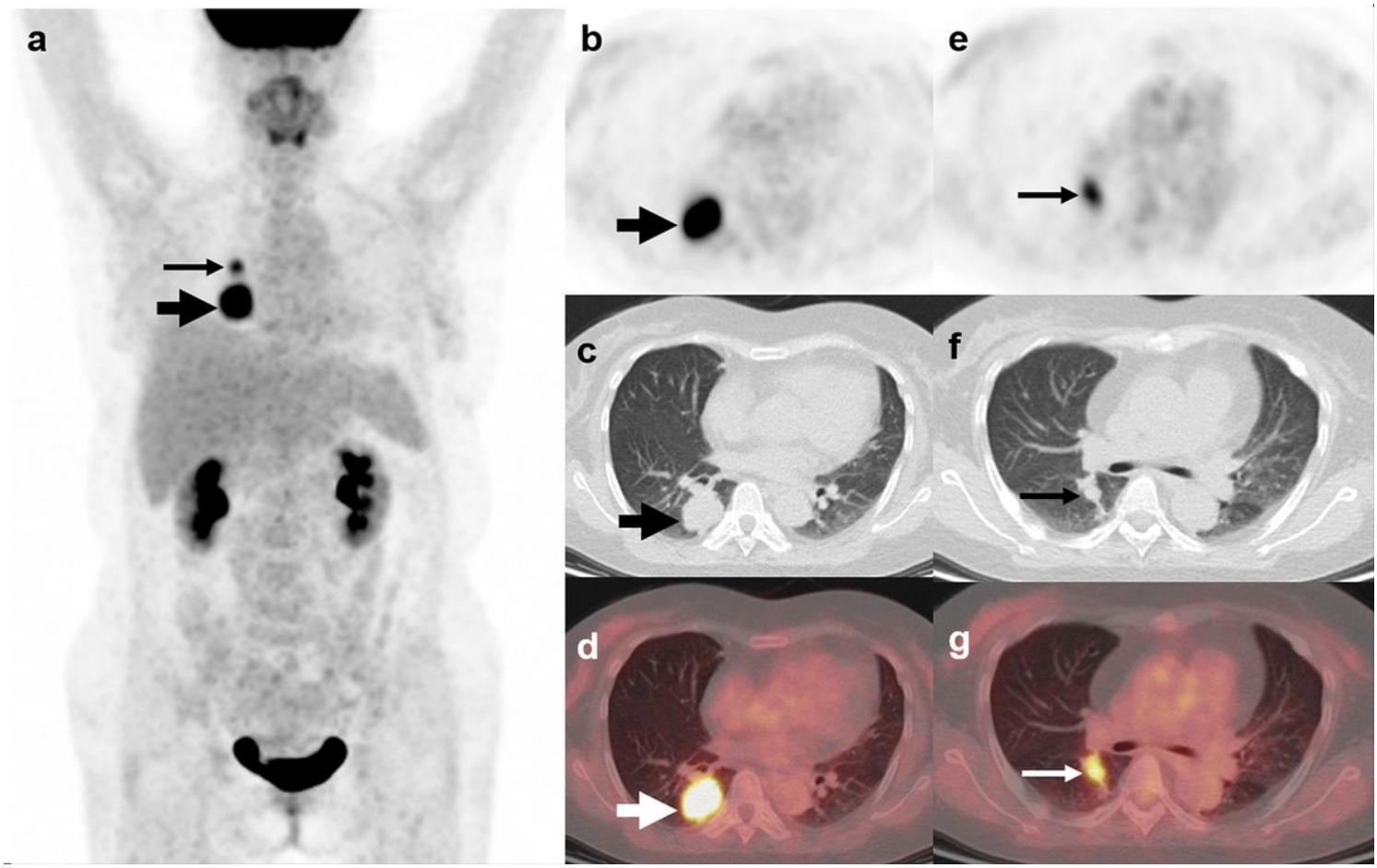

Figure 3

18F-FDG PET/CT findings in a representative case of cryptococcosis (Patient, 3). A 34-year-old woman with ectopic Cushing syndrome underwent 18F-FDG PET/CT for the detection of an adrenocorticotropic hormone-secreting tumor. Two FDG-avid lesions can be seen in the right lung (a–g; little arrows, SUVmax, 5.7; big arrows, SUVmax, 12.4). The two lesions were surgically removed. The pathological and immunohistochemical results indicated pulmonary cryptococcosis. 3 weeks after surgery, the patient's condition deteriorated showing severe headache and fever symptoms. Cryptococcus cerebrospinal culture was positive, suggesting cryptococcal meningitis. The patient responded poorly to the antibiotic therapy and died of a cerebral hernia.

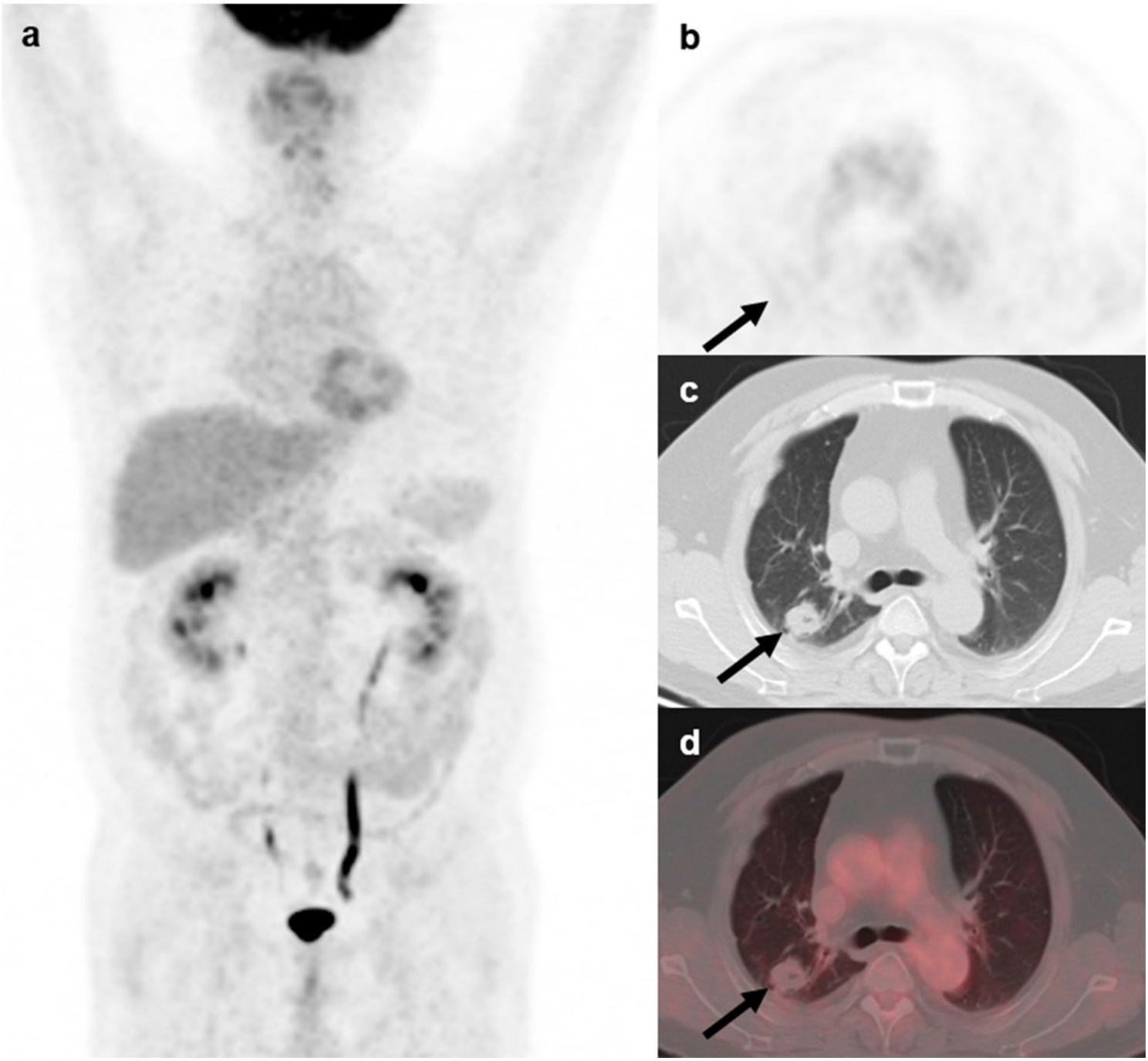

Figure 4

18F-FDG PET/CT in a representative case of aspergillosis (Patient, 4). A 39-year-old man diagnosed with ectopic Cushing syndrome underwent 18F-FDG PET/CT to search the primary lesion. PET/CT images presented a nodule in the right lung demonstrating slightly higher-than-background activity (arrows; SUVmax, 1.0). ACTH-secreting pulmonary carcinoid was suspected, while percutaneous lung biopsy confirmed a pulmonary aspergilloma.

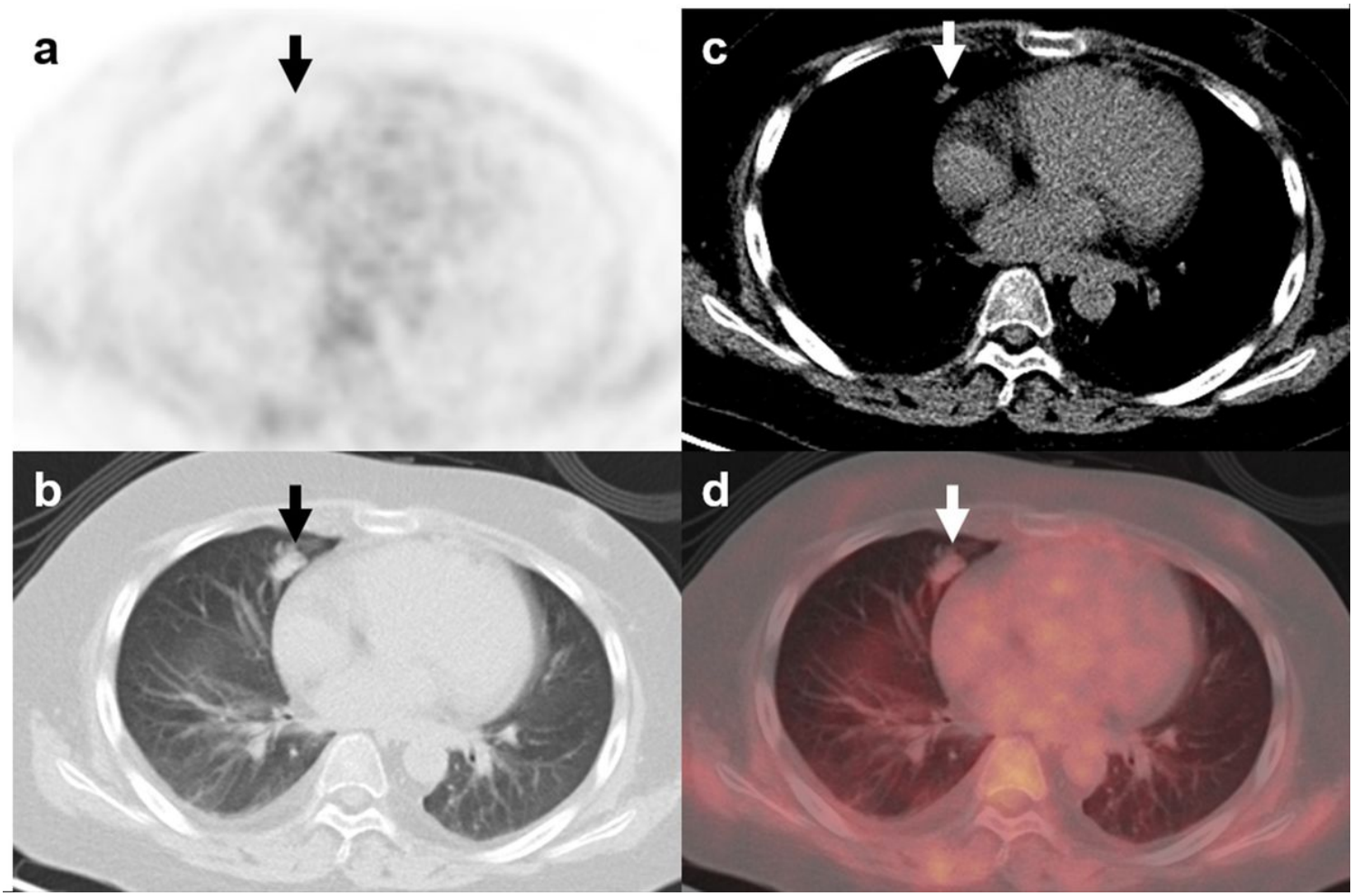

Figure 5

18F-FDG PET/CT findings in a representative case of an atypical carcinoid (Patient, 21). A 16-year-old man was diagnosed with ectopic Cushing syndrome. The patient underwent 18F-FDG PET/CT to localize the source of ACTH secretion. PET/CT images revealed a nodule with mild FDG activity (arrows; SUVmax, 1.1) in the right lung. The lesion was surgically removed, and histopathological analysis indicated an atypical carcinoid with ACTH positivity in immunohistochemistry.

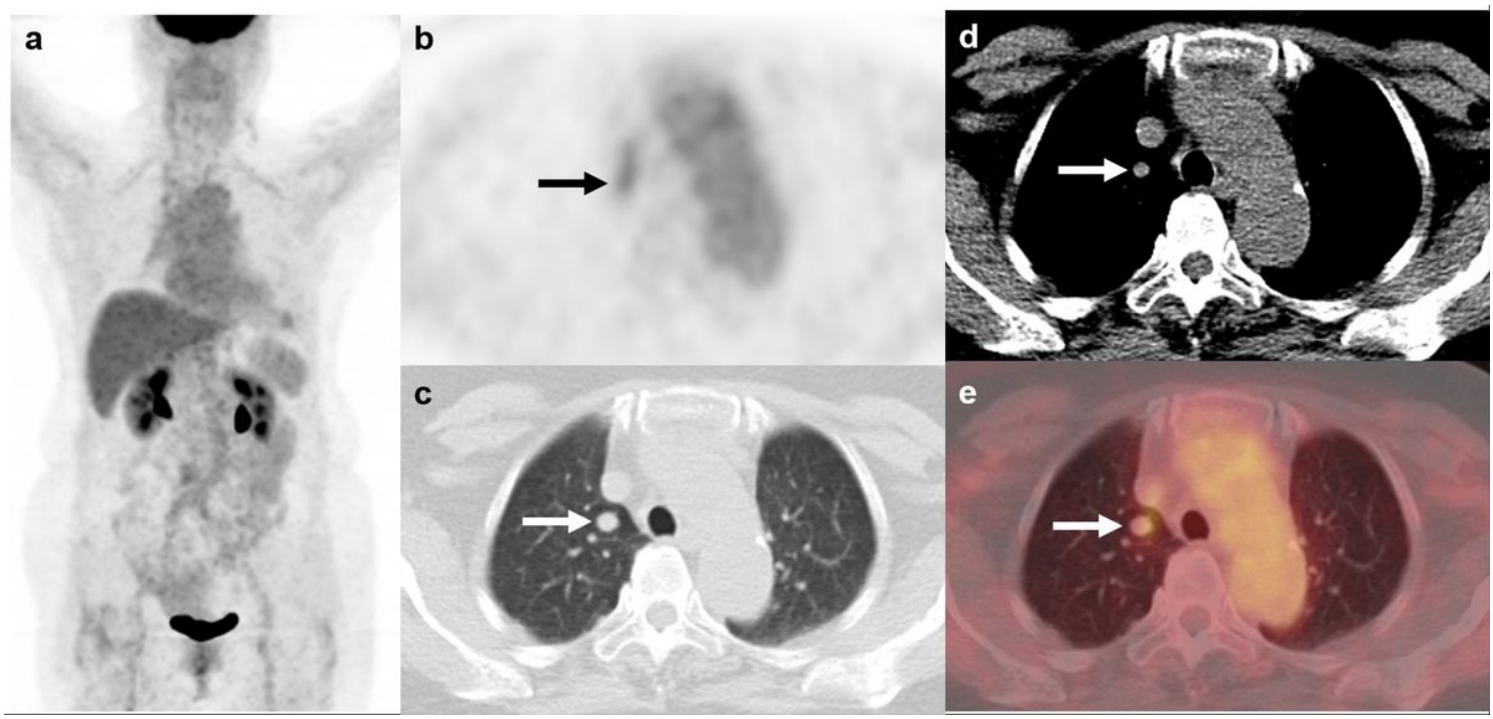

Figure 6

18F-FDG PET/CT findings in a representative case of a typical carcinoid (Patient, 17). A 72-year-old woman with ectopic Cushing syndrome received 18F-FDG PET/CT for the detection of an ACTH-secreting tumor. PET/CT images showed a nodule with slightly increased FDG uptake (arrows; SUVmax, 2.8) in the upper lobe of the right lung. Postoperative histopathology confirmed a typical carcinoid with positive ACTH immunostaining

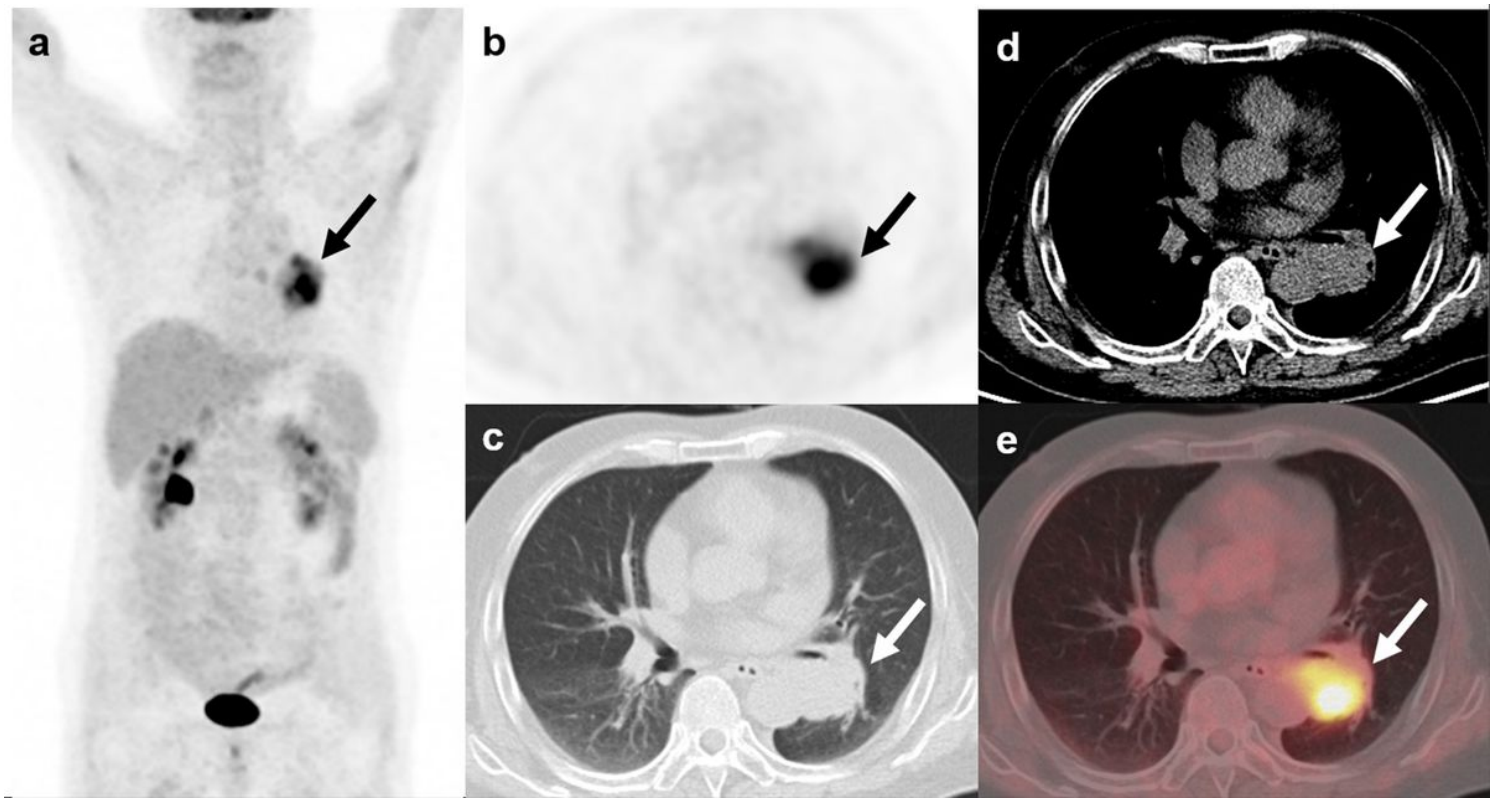

Figure 7

18F-FDG PET/CT findings in a representative case of small cell lung cancer (Patient, 24). A 57-year-old man diagnosed with ectopic Cushing syndrome underwent 18F-FDG PET/CT to search the primary tumor. PET/CT images demonstrate a mass with intense FDG uptake (arrows; SUVmax, 7.7) adjacent to the left hilum. Postoperative histopathology confirmed small cell lung cancer with ACTH positivity in immunohistochemistry.

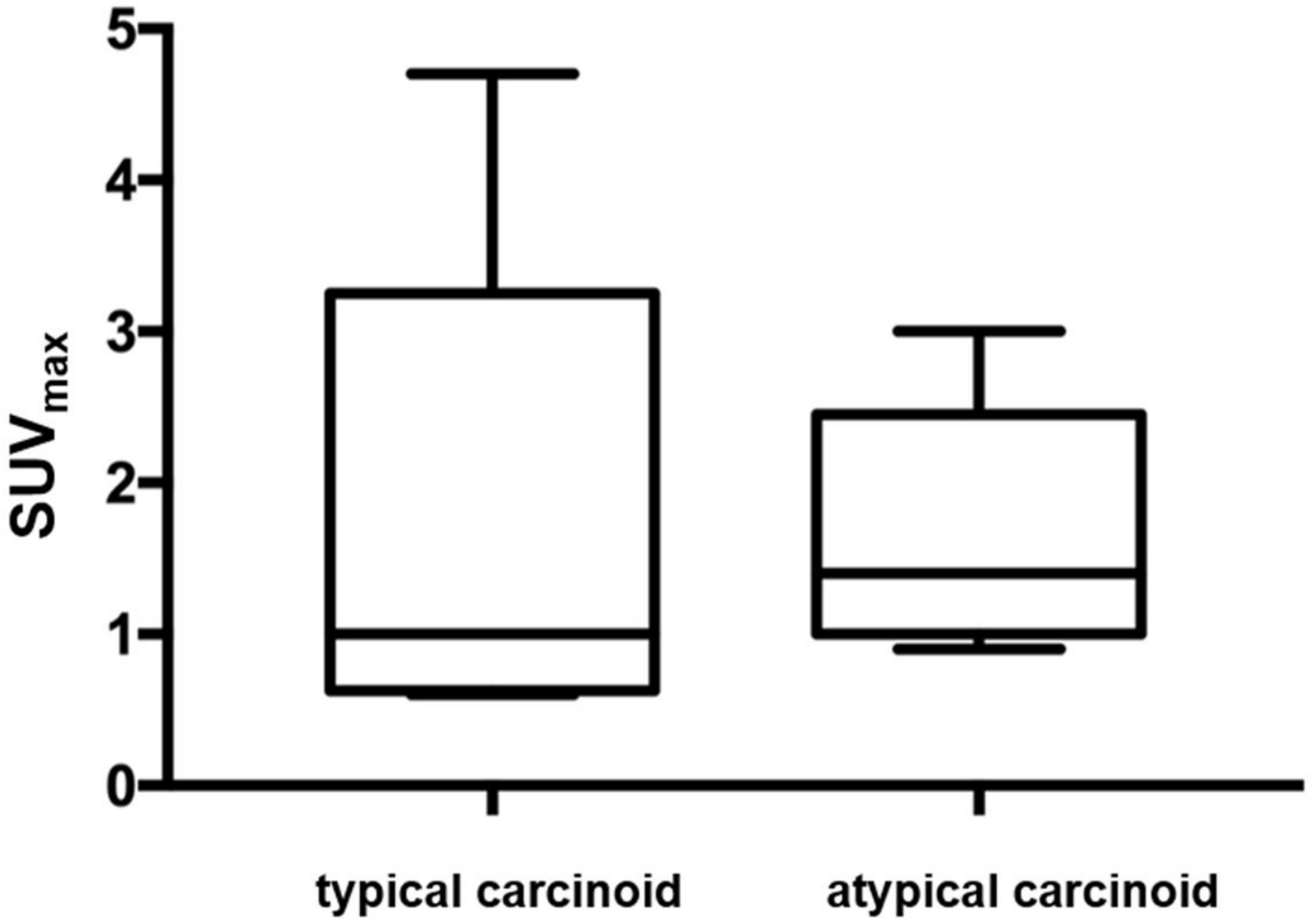

Figure 8

SUVmax difference between typical carcinoids and atypical carcinoids was not statistically significant (P = 0.597).

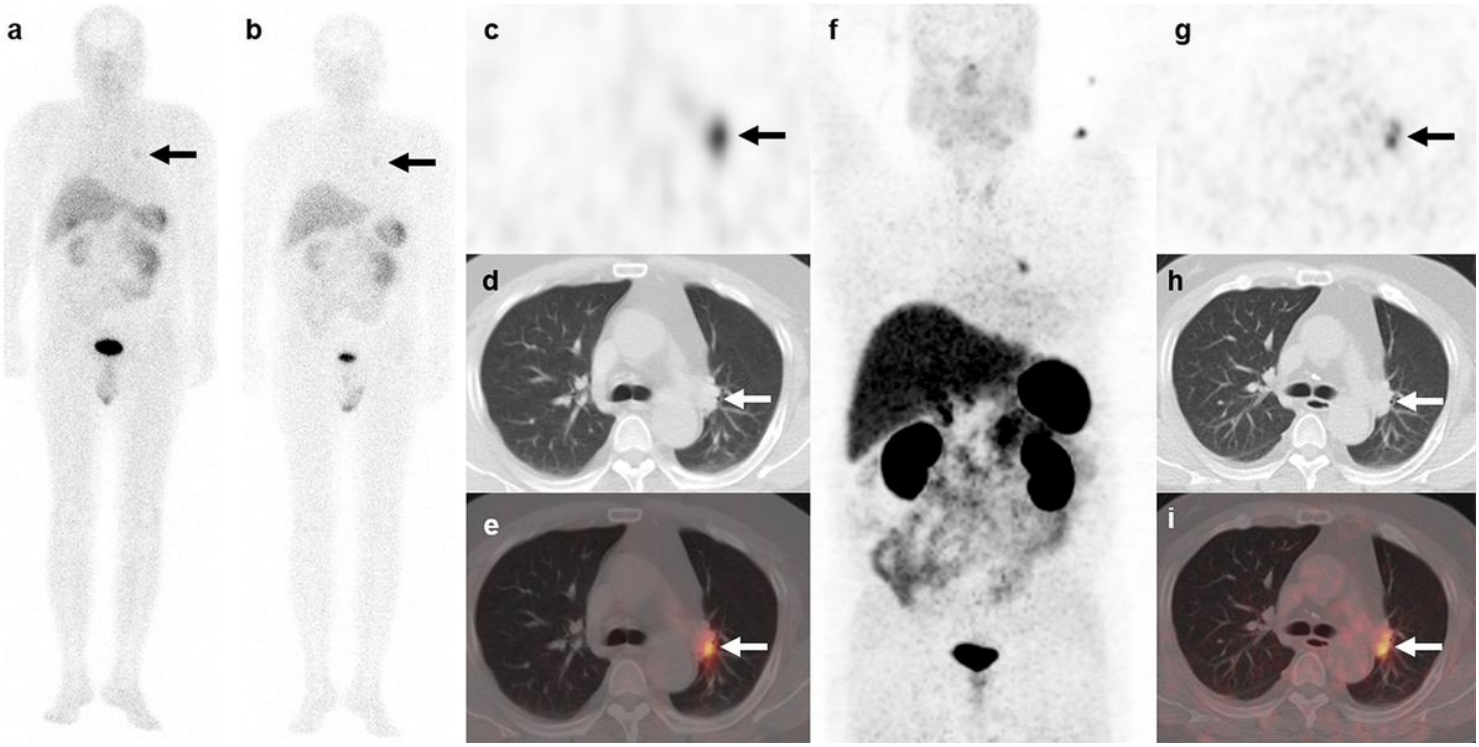

Figure 9

99mTc-HYNIC-TOC scintigraphy and 68Ga-DOTA-TATE PET/CT findings in a representative case of an atypical carcinoid (Patient, 15). A 45-year-old man with ectopic Cushing syndrome received 99mTc-HYNIC-TOC scintigraphy(a, 1 hour after injection; b, 4 hours after injection) and 68Ga-DOTA-TATE PET/CT for the detection of an ACTH-secreting tumor. 99mTc-HYNIC-TOC scintigraphy(c-e) and 68Ga-DOTA-TATE PET/CT (f-i) demonstrated a nodule with intense uptake (arrows) adjacent to the left hilum. Postoperative histopathology confirmed an atypical carcinoid with positive ACTH immunostaining. There were several body-surface radioactive contaminations in the left upper arm of the patient (f).